NIH Public Access
Author Manuscript
J Biomech. Author manuscript; available in PMC 2010 December 20.

Published in final edited form as:
J Biomech. 2010 April 19; 43(6): 1067–1073. doi:10.1016/j.jbiomech.2009.12.005.

Effects of enzymatic digestion on compressive properties of rat intervertebral discs

Ana Barbir[*], **Arthur J. Michalek**, **Rosalyn D. Abbott**, and **James C. Iatridis**
College of Engineering and Mathematical Sciences, University of Vermont, 33 Colchester Avenue, 207 Perkins Hall, Burlington, VT, 05405, USA

Abstract

Enzymatic treatments were applied to rat motion segments to establish structure–function relationships and determine mechanical parameters most sensitive to simulated remodeling and degeneration. Rat caudal and lumbar disc biomechanical behaviors were evaluated to improve knowledge of their similarities and differences due to their frequent use during in vivo models. Caudal motion segments were assigned to four groups: soaked (control), genipin treated, elastase treated, and collagenase treated. Fresh lumbar and caudal discs were also compared. The mechanical protocol involved five force-controlled loading stages: equilibration, cyclic compression-tension, quasi-static compression, frequency sweep, and creep. Crosslinking was found to have the greatest effect on IVD properties at resting stress. Elastin's role was greatest in tension and at higher force conditions, where GAG content was also a contributing factor. Collagenase treatment caused tissue compaction, which impacted mechanical properties at both high and low force conditions. Equilibration creep and cyclic compression-tension tests were the mechanical tests most sensitive to alterations in specific matrix constituents. Caudal and lumbar motion segments had many similarities but biomechanical differences suggested some distinctions in collagenous structure and water transport characteristics in addition to the geometric differences. Results provide a basis for interpreting biomechanical changes observed in animal model studies of degeneration and remodeling, and underscore the need to maintain and/or repair collagen integrity in IVD health and disease.

Keywords

Intervertebral; Elastin; Compression; Collagenase; Cross-linking

1. Introduction

Intervertebral disc (IVD) degeneration and aging involve substantial changes in composition and structure as well as altered mechanical properties (Adams and Roughley, 2006). Biochemically, IVD degeneration is accompanied by an increase in collagen crosslinking in the nucleus pulposus (Duance et al., 1998; Pokharna and Phillips, 1998), and an increase in the percentage of denatured type II collagen in the inner annulus fibrosus (AF) and nucleus pulposus (NP) (Antoniou et al., 1996) as well as changes in elastin content (Cloyd and Elliott, 2007; Johnson et al., 1985; Johnson et al., 1982). Collagenase damage to collagen

© 2009 Elsevier Ltd. All rights reserved.

[*] corresponding author: Tel.: +802 656 3902; fax: +802 656 3358. ana.barbir@uvm.edu (A. Barbir)..

Conflict of Interest Statement
None of the authors have conflicts of interest.

NIH-PA Author Manuscript
NIH-PA Author Manuscript
NIH-PA Author Manuscript

NIH-PA Author Manuscript

NIH-PA Author Manuscript

NIH-PA Author Manuscript

molecules is known to increase with aging and degeneration, but because of the extensive crosslinking this does not necessarily result in collagen loss (Roughley, 2004). Biomechanically, IVD degeneration is characterized by a decrease in intradiscal and osmotic pressure (Nachemson, 1960; Urban and McMullin, 1988), a reduced creep time constant (Kazarian, 1975; Koeller et al., 1986), increased AF compressive modulus (Iatridis et al., 1998), decreased annular tensile strength (Acaroglu et al., 1995), and decreased nucleus pulposus swelling pressure and effective aggregate modulus (Johannessen and Elliott, 2005). These changes tend to progress with increasing degenerative grade, yet a more direct relationship between these biomechanical and biochemical changes in the absence of disease process requires an animal model with fairly uniform structure and composition as well as interventions that are more specific than degeneration.

Degenerative and remodeling changes of soft-tissues may be simulated using targeted enzymatic treatments in vitro to make specific alterations to structure and content of molecular constituents. In articular cartilage, mechanical testing subsequent to targeted enzymatic digestion has demonstrated that collagen contributes to instantaneous and dynamic material responses while proteoglycans contribute to equilibrium stiffness (Bader et al., 1992; Korhonen et al., 2003; Laasanen et al., 2003; Mow et al., 1990; Park et al., 2008). In IVDs, increased collagen crosslinking has been demonstrated to increase tissue and/or motion segment stiffness in some studies (Chuang et al., 2007; Hedman et al., 2006; Wagner et al., 2006) while not affecting mechanical properties in others (Yerramalli et al., 2007). Collagenase digestion of IVDs has been infrequently used to assess structure–function relationships (Antoniou et al., 2006). Elastase treatment in isolated AF tissue was found to significantly increase transverse shear compliance (Michalek et al., 2009) and extensibility in radial tension (Smith et al., 2008). However, there has been no comprehensive study comparing effects of elastase, collagenase and a collagen cross-linker in a single highly controlled in vitro motion segment study.

IVD models of degeneration in rodents are appealing because of their high metabolic rates, high levels of experimental control, availability and relatively low cost. Caudal and lumbar IVDs generally have similar compression and torsion stiffness yet differences were noted in neutral zone and viscoelastic behaviors that may be associated with geometric and material differences between levels (Beckstein et al., 2008; Elliott and Sarver, 2004; Espinoza Orias et al., 2009). Inherent nonlinearities in material behaviors can suggest that structural biomechanical difference may be more (or less) pronounced when evaluated under different levels of axial preloads (Patwardhan et al., 1999; Quint and Wilke, 2008). Consequently, in this study it was important to compare lumbar and caudal rat IVD properties under simulated in vivo ‘resting stress’ conditions.

The aim of this study was to comprehensively investigate relationships between biomechanical behavior of the IVD and chemical alterations to collagen and elastin structure and content. Rat caudal and lumbar IVD biomechanical behaviors were also tested to evaluate geometric effects and enhance current knowledge of their similarities and differences due to their frequent use during in vivo studies. We hypothesized that (1) collagen and elastin have distinct mechanical roles in determining the viscoelastic and elastic behaviors of rat IVDs; and (2) lumbar and caudal IVDs will exhibit similar viscoelastic and elastic behaviors when tested under simulated in vivo resting stress conditions.

NIH-PA Author Manuscript

NIH-PA Author Manuscript

NIH-PA Author Manuscript

2. Methods

2.1. Sample preparation

Caudal and lumbar motion segments (60 for biomechanics; 60 for biochemistry) were harvested from skeletally mature Sprague–Dawley rats obtained from IACUC approved protocols. Three caudal vertebra-disc-vertebra motion segments (c5-6, c7-8, c9-10) were harvested from 34 rats and a single lumbar motion segment (L3-4) was harvested from 10 rats. To harvest tail motion segments, the skin and tendons were removed as well as any remaining soft tissue. Lumbar motion segments were dissected, and posterior elements were removed. Caudal and lumbar motion segments were wrapped in PBS soaked gauze, immediately following dissection, flash frozen in liquid nitrogen and stored at −80 °C. On the day of testing, mechanical test specimens were thawed and potted in 12.5mm diameter stainless steel tubes using cyanoacrylate, and a custom clamp to insure motion segments were centered within pots and the superior–inferior axis of the disc was parallel with the loading axis, as described (Masuoka et al., 2007).

2.2. Biochemical Treatments

Biomechanical specimens were systematically assigned across levels to one of four treatment groups (n=10 per group). Immediately following potting, motion segments were either mechanically tested (fresh lumbar and caudal), or subjected to a chemical treatment (Groups I–IV). Pins were attached (Fig. 1.) to hold the distance between pots constant and minimize axial swelling and the treatments were carried out for 12 h at 37 °C in 4 mL of solution:

- **I.** Soaked (Control): soaked in PBS,
- **II.** Elastase treated: soaked in 3U of pancreatic Elastase (E1250, Sigma-Aldrich) in 1 mL of 0.2 M Tris–HCl, pH 8.6, with 10 mM N-ethylmaleimide and 5 mM benzamidine hydrochloride as protease inhibitors (Smith et al., 2008)
- **III.** Collagenase treated: soaked in 800U of collagenase (C7657, Sigma-Aldrich) in 0.15 M PBS, pH 7.1;
- **IV.** Genipin treated: soaked in 1% Genipin (07-03021, Wako) in 0.15 M PBS.

Biochemical specimens used 60 caudal IVDs with n=15 per treatment group (I-IV).

2.3. Biomechanical testing

Potted specimens were tested in an Enduratec ELF 3200 (Bose Corporation) using custom grips (MacLean et al., 2007). The test protocol (Fig. 2) was followed for each group in a fluid bath consisting of a PBS solution with protease inhibitors (1 μg/mL Pepstatin-A, 1 mM EDTA, 1 mM N-ethylmaleimide, 1 mM benzamidine). The mechanical test consisted of 5 force-controlled loading stages: (A) equilibration, (B) cyclic compression-tension, (C) quasi-static compression, (D) frequency sweep, and (E) creep. Stage A consisted of a 30 min dwell at −1.875 N. This equilibrium compression load magnitude was chosen based on average rat tail disc geometry (diameter: 4 mm, height: 0.8 mm) and target rat tail IVD resting stress of 0.15 MPa compression (MacLean et al., 2005), which served as a baseline for all subsequent tests. Stage B included sinusoidal tension-compression for 20 cycles at 1 Hz with a 6.25 N amplitude centered about −1.875 N. Stage C subjected the specimens to a slow compressive ramp at 0.005 N/s from −1.875 to −8.125 N, while stage D consisted of 5 cycles at six different frequencies: 0.05, 0.1, 0.5, 1, 5, and 10 Hz applied from −1.875 to −8.125 N in sinusoidal compression. The final stage E consisted of a 12.5 N dwell for 30 min.

NIH-PA Author Manuscript

NIH-PA Author Manuscript

NIH-PA Author Manuscript

2.4. Biochemical assays

Biomechanical (following testing) and biochemical test specimens were flash frozen in liquid nitrogen, whole IVDs were dissected from vertebrae and wet tissue weights measured. Samples were then lyophilized to obtain dry weights, and water content was calculated. IVDs for biochemical analysis were rehydrated and digested in 250 μL of each α-chymotrypsin and Proteinase K (1 mg/ml in 50 mM Tris–HCl pH 7.6 from Sigma, St. Louis, MO) at 37 and 56 °C, respectively. The α-chymotrypsin and proteinase K digests were analyzed separately and color-imetrically assayed for hydroxyproline content, free amino acid content and GAG content (n=5 per treatment group) to asses changes in the amount of collagen, crosslinks and proteoglycans, respectively. The total collagen was quantified through a hydroxyproline assay (Reddy and Enwemeka, 1996), and amount of degraded collagen was calculated from hydroxyproline in the α-chymotrypsin digest relative to total collagen in both digests. An adapted ninhydrin assay measured free amines per mole of collagen (Moore and Stein, 1954) which increase as proteins are degraded and decrease as more free amines are used for crosslinking. GAG content per dry weight was determined using the dimethylmethylene blue (DMMB) method (Farndale et al., 1986).

2.5. Data Analysis

A custom MATLAB (Mathworks) code analyzed data at each test stage to compute relevant mechanical parameters. For stages A and E, the creep displacement, d, was fit to a stretched exponential function (Lakes, 1998),

$$d = (d_\infty - d_o)\left[1 - e^{-(t/\tau)^\beta}\right]$$

where $(d_\infty - d_0)$ is the equilibrium height loss, t is time, τ is a time constant and β is a stretch constant. Motion segment height loss from the beginning to end of each creep stage was also measured. From stage B, the cyclic compression-tension test, three dynamic stiffness values (compression, neutral zone and tension) as well as a neutral zone length were calculated using a trilinear fit (Sarver and Elliott, 2005) to force–displacement data from the average of the of the 18th and 19th loading and unloading cycles. Neutral zone length was defined by the distance between the intersection points of the neutral line with the tension and compression lines. In stage C, quasi-static stiffness was determined by linear regression of force–displacement data. In stage D, the dynamic stiffness (K*) and the phase angle (δ) were calculated from

$$K^* = \left(\frac{F_0}{d_0}\right)e^{i\delta} \text{ and } \delta = \sin^{-1}\left(\frac{1}{2\pi}\int_{t_0}^{t_0+T} F\frac{\mathrm{d}d}{\mathrm{d}t}\mathrm{d}t\right)$$

where F is force, d is displacement, T is period and t is time (Findley et al., 1989).

2.6. Statistical Analysis

Statistical analyses involved one-way analysis of variances (ANOVAs) followed by Fisher's protected least-significant difference (Fisher's PLSD). For comparisons of spinal level (caudal vs. lumbar), Student's t-test was used. All statistical analyses were performed using Statview (SAS Institute Inc., NC), with $p<0.05$ significant, presented as means±SEM.

3. Results

Significant variations in mechanical parameters due to chemical treatment (Table 1) and spinal region (Table 2) were measured. In all groups, no significant effects of frequency

NIH-PA Author Manuscript

NIH-PA Author Manuscript

NIH-PA Author Manuscript

were detected and dynamic stiffness and phase angle results are presented from the 1 Hz data. There were no significant differences in water content between any of the treated groups and control, with 68% average water for the biomechanical test specimens (measured post testing) and 80% for the biochemical specimens.

Elastase treatment caused changes in elastic and viscoelastic motion segment mechanical properties with a 17% decrease in tensile stiffness during cyclic tension-compression (B) and a 44% decrease in equilibrium height loss ($d_\infty - d_0$) during creep (E). Collagenase treatment affected mechanical parameters in all but one stage of testing (C). We computed a significant 10% increase in the stretch constant β for the equilibration stage (A), an 18% increase in neutral zone length during cyclic tension-compression (B) and a significant increase in dynamic stiffness for all frequencies during the frequency sweep (D). The collagenase treated group also exhibited a significant 36% decrease in the equilibrium height loss ($d_\infty - d_0$) and a 39% decrease in the time constant τ during the creep stage (E). Genipin treatment caused a significant 62% decrease in equilibrium height loss ($d_\infty - d_0$) and a 19% increase in the stretch constant β. In the compression-tension stage (B), genipin increased neutral zone stiffness by 965% and reduced its length by 58% relative to control. Tensile stiffness significantly decreased by 43%, although no significant changes in frequency sweep or creep stages were detected from genipin treatment.

Biochemical analysis of soaked control found 88.5±15.5 μg hydroxyproline/mg dry tissue, 0.31±0.06 μmoles free amines/μmoles collagen, and 47.5±6.6 μg GAG/mg dry tissue. Treatments modified biochemical content from the PBS control (Table 3) with elastase causing 23.4% decrease in hydroxyproline content, 37.7% increase in free amines, and 32% decrease in GAG. Collagenase treatment decreased hydroxyproline content, and increased free amines and GAG. Genipin treatment decreased free amines by 37.2%, although GAG and hydroxyproline content could not be measured because natural color of genipin confounded the colorimetric assays.

No significant differences were found between lumbar and caudal motion segments in quasi-static stiffness, tensile or compressive stiffness, dynamic stiffness, phase angle, or creep height loss (Table 2). Significant differences in the equilibration stage included a 46% and 39% lower equilibrium and measured height loss respectively in lumbar motion segments relative to caudal. In the compression-tension stage, the neutral zone of the lumbar disc was significantly stiffer by 693% and had a significantly shorter neutral zone by 48% than caudal segments. In the creep stage (E), the lumbar IVD exhibited a significantly lower equilibrium height loss, time constant and stretch constant by 38%, 57% and 9%, respectively.

4. Discussion

Enzymatic treatments were applied to rat motion segments to establish structure–function relationships and determine those mechanical parameters expected to be sensitive to simulated remodeling and degeneration. Minimization of IVD swelling during enzyme treatments, maintenance of resting stress during biomechanical testing, and the quantification of biochemical treatments were considered important features of the testing protocol. In support of the first hypothesis, collagenase and elastase treatments resulted in distinct mechanical responses. In support of the second hypothesis, lumbar and caudal IVDs exhibited similar compressive, tensile, and dynamic stiffness behaviors, however, some differences in neutral zone and creep behaviors were also determined.

Genipin treatment decreased the number of free amines, indicating an increase in crosslinking (Table 3). This decreased neutral zone length, increased neutral zone stiffness (Fig. 3), and decreased creep during the initial equilibration stage (Fig. 4). Neutral zone was

NIH-PA Author Manuscript

NIH-PA Author Manuscript

NIH-PA Author Manuscript

most sensitive to genipin treatment, so we conclude that crosslinking affects matrix stiffness and water transport under low force conditions. Genipin treatment also decreased equilibration creep and strongly affected compression-tension testing (Stages A and B), while not contributing to the test stages performed under higher force pointing to a greater effect of crosslinking under physiological resting stress.

Elastase treatment increased free amines, while decreasing GAG content, and having no measurable effect on hydroxyproline (Table 3). While elastase content was not measured directly, the same elastase degradation protocol (Smith et al., 2008) caused a 68% degradation of elastin in human AF samples. In this study the increase in free amines with no effect on hydroxyproline implies that a large amount of protein other than collagen was degraded. Although elastin contains hydroxyproline, we assume it is too small to be measured in rat IVDs, since hydroxyproline accounts for 1% of elastin (Osman et al., 1980), and elastin accounts for 2% of IVD dry weight (Cloyd and Elliott, 2007). Elastase treatment significantly decreased tensile stiffness (Fig. 3) and height loss during final creep (Fig. 4b), suggesting a more important role for elastin at higher load magnitudes. Mechanically, elastin has also been implicated in fiber recruitment in transverse shear (Michalek et al., 2009) and radial tension (Smith et al., 2008). The impact of elastase treatment in this study was found mostly in tension, while in compression the decrease in height loss during creep can be attributed to the loss of GAG.

Collagenase treatment decreased hydroxyproline content and increased free amines and GAG content. The apparent increase in GAG content was due to a 43% decrease in dry weight of the collagenase treated group compared to control, which was used as a normalization factor. The loss of fiber integrity due to decreased hydroxyproline content led to an increased neutral zone (Fig. 3). The increase in dynamic stiffness can be explained by tissue compaction at both low and high loads which causes the tissue to be loaded under a stiffer portion of the nonlinear load-deformation curve. The concept of tissue compaction following loss of fiber integrity may be consistent with the reported increased compressive modulus of human AF tissue associated with disc degeneration (Iatridis et al., 1998). In this study, the increase in compaction was consistent with the significantly lower cumulative height loss and shorter creep time constant in the collagenase-treated group.

No significant differences were observed between caudal and lumbar motion segments for compressive or tensile stiffness, quasi-static stiffness, dynamic stiffness, or phase angle. However, neutral zone variations between rat lumbar and caudal discs were observed consistent with previously findings (Elliott and Sarver, 2004). In addition, creep equilibrium displacement and time constant were significantly lower for lumbar compared to caudal IVDs. Differences in geometry between lumbar and caudal IVDs (lumbar IVD diameter: 3.5 mm, height: 0.64 mm vs. caudal IVD diameter: 4 mm, height 0.8 mm) only partially account for these biomechanical differences. We conclude that caudal and lumbar motion segments have many similarities but that biomechanical differences suggested distinct collagenous structure and water transport characteristics in addition to the clear geometric differences.

Some limitations are notable. Collagen and elastin content, as well as crosslinking changes occur with degeneration, yet in this study those changes were induced chemically and not physiologically. The interventions in this study are intended to help improve understanding and interpretation of remodeling changes observed in small animal models and not intended as a clinical model of degeneration. The soaked condition served as control since all treatments required a soaking period. The reduction in tensile stiffness of the crosslinked group was associated with relatively few points in the linear tension zone of the cyclic compression-tension stage. This was a result of the maximum tensile force of only 4.375 N (considered reasonable since there is little axial tensile loading on IVDs) and a relatively

NIH-PA Author Manuscript

NIH-PA Author Manuscript

NIH-PA Author Manuscript

high neutral zone stiffness. The blue color of genipin crosslinks interfered with some colorimetric assays, preventing measurements for DMMB and hydroxyproline.

In conclusion, this study determined specific IVD properties in compression that were sensitive to the content and structure of collagen, elastin, and IVD geometry. Crosslinking was found to have the greatest effect on IVD properties at resting stress. Elastin's role was greatest in tension and at higher force conditions, where GAG content was also a contributing factor. Collagenase treatment caused tissue compaction, which impacted mechanical properties at both high and low force conditions. Results also indicated that equilibration creep and cyclic compression-tension tests were the mechanical tests most sensitive to alterations in specific matrix constituents. The structure–function relationships reported provide a basis for interpreting biomechanical changes observed in animal model studies of degeneration and remodeling, and underscore the need to maintain and/or repair collagen integrity in IVDs.

Acknowledgments

We gratefully acknowledge helpful conversations with Dr. Martin Case. This work was funded by NIH: 1R01AR051146, and NASA/VSGC: NNX07AK92A

References

Acaroglu ER, Iatridis JC, Setton LA, Foster RJ, Mow VC, Weidenbaum M. Degeneration and aging affect the tensile behavior of human lumbar anulus fibrosus. Spine 1995;20:2690–2701. [PubMed: 8747247]

Adams MA, Roughley PJ. What is intervertebral disc degeneration, and what causes it? [Review]. Spine 2006;31:2151–2161. [PubMed: 16915105]

Antoniou J, Mwale F, Demers CN, Beaudoin G, Goswami T, Aebi M, Alini M. Quantitative magnetic resonance imaging of enzymatically induced degradation of the nucleus pulposus of intervertebral discs. Spine 2006;31:1547–1554. [PubMed: 16778686]

Antoniou J, Steffen T, Nelson F, Winterbottom N, Hollander AP, Poole RA, Aebi M, Alini M. The human lumbar intervertebral disc . evidence for changes in the biosynthesis and denaturation of the extracellular matrix with growth, maturation, ageing, and degeneration. Journal of Clinical Investigation 1996;98:996–1003. [PubMed: 8770872]

Bader DL, Kempson GE, Egan J, Gilbey W, Barrett AJ. The effects of selective matrix degradation on the short-term compressive properties of adult human articular cartilage. Biochimica et Biophysica Acta (BBA)—General Subjects 1992;1116:147–154.

Beckstein JC, Sen S, Schaer TPV, Vresilovic EJ, Elliott DM. Comparison of Animal Discs Used in Disc Research to Human Lumbar Disc: Axial Compression Mechanics and Glycosaminoglycan Content. Spine 2008;33:E166–E173. [PubMed: 18344845]

Chuang S-Y, Odono RM, Hedman TP. Effects of exogenous crosslinking on in vitro tensile and compressive moduli of lumbar intervertebral discs. Clinical Biomechanics 2007;22:14–20. [PubMed: 17005305]

Cloyd JMBA, Elliott DMP. Elastin content correlates with human disc degeneration in the anulus fibrosus and nucleus pulposus. Spine 2007;32:1826–1831. [PubMed: 17762289]

Duance VC, Crean JKG, Sims TJ, Avery N, Smith S, Menage J, Eisenstein SM, Roberts S. Changes in collagen cross-linking in degenerative disc disease and scoliosis. Spine 1998;23:2545–2551. [PubMed: 9854753]

Elliott DM, Sarver JJ. Young investigator award winner: validation of the mouse and rat disc as mechanical models of the human lumbar disc. Spine 2004;29:713–722. [PubMed: 15087791]

Espinoza Orias AA, Malhotra NR, Elliott DM. Rat disc torsional mechanics: effect of lumbar and caudal levels and axial compression load. Spine Journal 2009;9:204–209. [PubMed: 18495544]

NIH-PA Author Manuscript

NIH-PA Author Manuscript

NIH-PA Author Manuscript

Farndale RW, Buttle DJ, Barrett AJ. Improved quantitation and discrimination of sulphated glycosaminoglycans by use of dimethylmethylene blue. Biochimica et Biophysica Acta 1986;883:173–177. [PubMed: 3091074]

Findley, WN.; Lai, JS.; Onaran, K. Linear viscoelastic constitutive equations, Creep and Relaxation in Nonlinear Viscoelastic Materials. Dover; New York: 1989. p. 90-96.

Hedman TP, Saito H, Vo CB, Chuang S-Y. Exogenous cross-linking increases the stability of spinal motion segments. Spine 2006;31:E480–E485. [PubMed: 16816747]

Iatridis JC, Setton LA, Foster RJ, Rawlins BA, Weidenbaum M, Mow VC. Degeneration affects the anisotropic and nonlinear behaviors of human anulus fibrosus in compression. Journal of Biomechanics 1998;31:535–544. [PubMed: 9755038]

Johannessen W, Elliott DM. Effects of degeneration on the biphasic material properties of human nucleus pulposus in confined compression. Spine 2005;30:E724–E729. [PubMed: 16371889]

Johnson EF, Berryman H, Mitchell R, Wood WB. Elastic fibres in the anulus fibrosus of the adult human lumbar intervertebral disc. A preliminary report. Journal of Anatomy 1985;143:57–63. [PubMed: 3870732]

Johnson EF, Chetty K, Moore IM, Stewart A, Jones W. The distribution and arrangement of elastic fibres in the intervertebral disc of the adult human. Journal of Anatomy 1982;135:301–309. [PubMed: 7174505]

Kazarian LE. Creep characteristics of the human spinal column. Orthopedic Clinics of North America 1975;6:3–18. [PubMed: 1113976]

Koeller W, Muehlhaus S, Meier W, Hartmann F. Biomechanical properties of human intervertebral discs subjected to axial dynamic compression—Influence of age and degeneration. Journal of Biomechanics 1986;19:807–816. [PubMed: 3782163]

Korhonen RK, Laasanen MS, Toyras J, Lappalainen R, Helminen HJ, Jurvelin JS. Fibril reinforced poroelastic model predicts specifically mechanical behavior of normal, proteoglycan depleted and collagen degraded articular cartilage. Journal of Biomechanics 2003;36:1373–1379. [PubMed: 12893046]

Laasanen MS, Töyräs J, Korhonen RK, Rieppo J, Saarakkala S, Nieminen MT, Hirvonen J, Jurvelin JS. Biomechanical properties of knee articular cartilage. Biorheology 2003;40:133–140. [PubMed: 12454397]

Lakes, RS. Constitutive relations. In: Kulacki, FA., editor. Viscoelastic Solids. CRC Press; Boca Raton: 1998. p. 15-62.

MacLean JJ, Lee CR, Alini M, Iatridis JC. The effects of short-term load duration on anabolic and catabolic gene expression in the rat tail inter-vertebral disc. Journal of Orthopaedic Research 2005;23:1120–1127. [PubMed: 16140193]

MacLean JJ, Owen JP, Iatridis JC. Role of endplates in contributing to compression behaviors of motion segments and intervertebral discs. Journal of Biomechanics 2007;40:55–63. [PubMed: 16427060]

Masuoka K, Michalek AJ, MacLean JJ, Stokes IA, Iatridis JC. Different effects of static versus cyclic compressive loading on rat intervertebral disc height and water loss in vitro. Spine 2007;32:1974–1979. [PubMed: 17700443]

Michalek AJ, Buckley MR, Bonassar LJ, Cohen I, Iatridis JC. Measurement of local strains in intervertebral disc anulus fibrosus tissue under dynamic shear: contributions of matrix fiber orientation and elastin content. Journal of Biomechanics 2009;42:2279–2285. [PubMed: 19664773]

Moore S, Stein WH. A modified ninhydrin reagent for the photometric determination of amino acids and related compounds. Journal of Biological Chemistry 1954;211:907–913. [PubMed: 13221596]

Mow, VC.; Fithian, DC.; Kelly, MA. Fundamentals of articular cartilage and meniscus biomechanics. In: Ewing, JW., editor. Articular Cartilage and knee Joint Function: Basic Science and Arthroscopy. Raven Press; New York: 1990. p. 1-18.

Nachemson A. Lumbar intradiscal pressure. Experimental studies on postmortem material. Acta Orthopaedica Scandinavica Supplement 1960;43:1–104. [PubMed: 14425680]

NIH-PA Author Manuscript

NIH-PA Author Manuscript

NIH-PA Author Manuscript

Osman M, Keller S, Cerreta JM, Leuenberger P, Mandl I, Turino GM. Effect of papain-induced emphysema on canine pulmonary elastin. Proceeding of the Society for Experimental Biology and Medicine 1980;164:471–477.

Park S, Nicoll S, Mauck R, Ateshian G. Cartilage mechanical response under dynamic compression at physiological stress levels following collagenase digestion. Annals of Biomedical Engineering 2008;36:425–434. [PubMed: 18193355]

Patwardhan AG, Havey RM, Meade KP, Lee B, Dunlap B. A follower load increases the load-carrying capacity of the lumbar spine in compression. Spine 1999;24:1003–1009. [PubMed: 10332793]

Pokharna HK, Phillips FM. Collagen crosslinks in human lumbar intervertebral disc aging. Spine 1998;23:1645–1648. [PubMed: 9704370]

Quint U, Wilke HJ. Grading of degenerative disk disease and functional impairment: imaging versus patho-anatomical findings. European Spine Journal 2008;17:1705–1713. [PubMed: 18839226]

Reddy GK, Enwemeka CS. A simplified method for the analysis of hydroxyproline in biological tissues. Clinical Biochemistry 1996;29:225–229. [PubMed: 8740508]

Roughley PJ. Biology of intervertebral disc aging and degeneration: involvement of the extracellular matrix. Spine 2004;29:2691–2699. [PubMed: 15564918]

Sarver JJ, Elliott DM. Mechanical differences between lumbar and tail discs in the mouse. Journal of Orthopaedic Research 2005;23:150–155. [PubMed: 15607887]

Smith L, Byers S, Costi J, Fazzalari N. Elastic fibers enhance the mechanical integrity of the human lumbar anulus fibrosus in the radial direction. Annals of Biomedical Engineering 2008;36:214–223. [PubMed: 18066662]

Urban JPG, McMullin JF. Swelling Pressure of the Lumbar Intervertebral Discs: Influence of Age, Spinal Level, Composition, and Degeneration. Spine 1988;13:179–187. [PubMed: 3406838]

Wagner DR, Reiser KM, Lotz JC. Glycation increases human annulus fibrosus stiffness in both experimental measurements and theoretical predictions. Journal of Biomechanics 2006;39:1021–1029. [PubMed: 15878594]

Yerramalli C, Chou A, Miller G, Nicoll S, Chin K, Elliott D. The effect of nucleus pulposus crosslinking and glycosaminoglycan degradation on disc mechanical function. Biomechanics and Modeling in Mechanobiology 2007;6:13–20. [PubMed: 16715318]

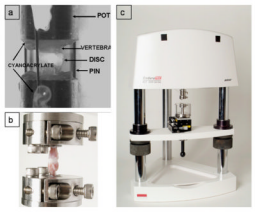

Fig. 1.

(a) Example motion segment potted and pinned to prevent swelling prior to chemical treatment, (b) Motion segment attached to the loading apparatus with custom grips, (c) Experimental loading apparatus with a fluid chamber, a 3-axis positioning stage and custom grips.

NIH-PA Author Manuscript
NIH-PA Author Manuscript
NIH-PA Author Manuscript

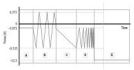

Fig. 2.
Mechanical protocol where stage A is equilibration, B is cyclic compression-tension, C is quasi-static compression, D is dynamic compression at 1 Hz, and E is creep.

NIH-PA Author Manuscript
NIH-PA Author Manuscript
NIH-PA Author Manuscript

NIH-PA Author Manuscript

NIH-PA Author Manuscript

NIH-PA Author Manuscript

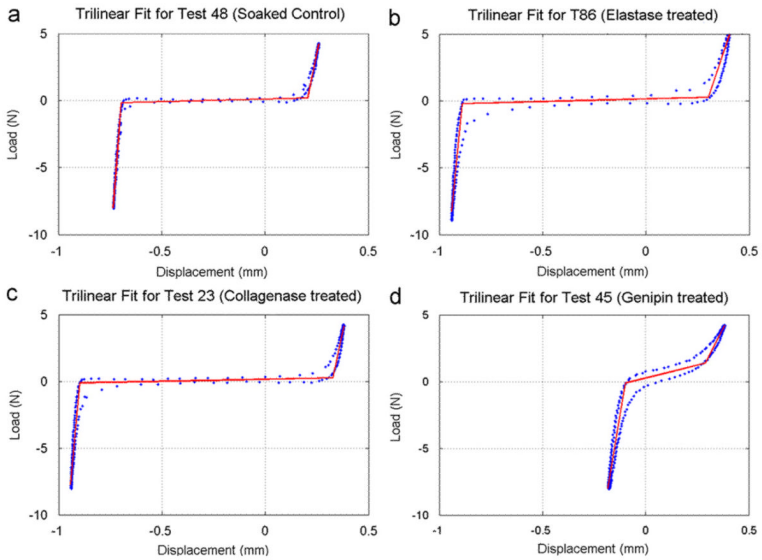

Fig. 3.

Sample trilinear fits to data from the compression-tension conditioning stage, illustrating representative differences between (a) Soaked (Control), (b) elastase treated, (c) Collagenase treated and (d) genipin-treated IVD.

NIH-PA Author Manuscript

NIH-PA Author Manuscript

NIH-PA Author Manuscript

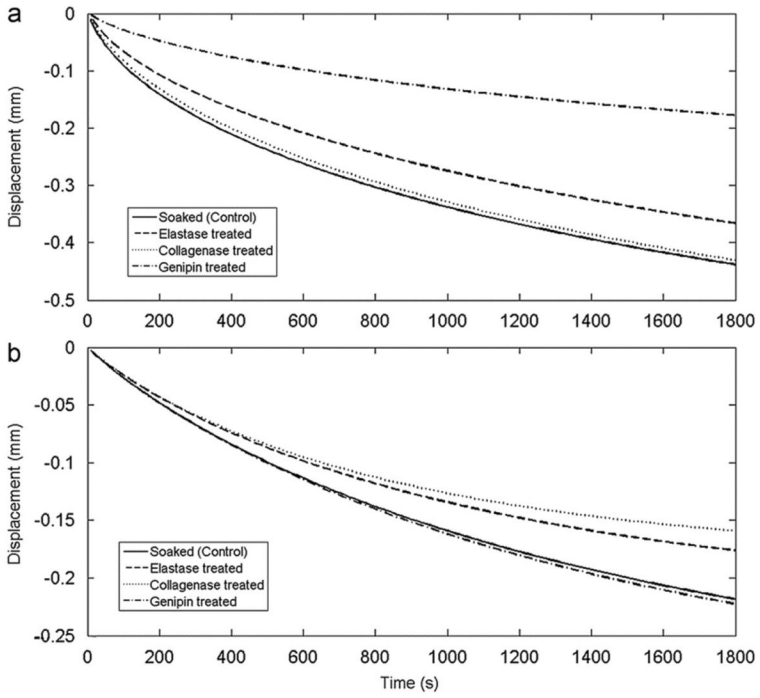

Fig. 4.

Transient deformation patters of (a) equilibration (stage A) at 0.15 MPa and (b) creep (stage E) at 1 MPa for simulated stretched exponential fit using mean parameters for each experimental group.

NIH-PA Author Manuscript NIH-PA Author Manuscript NIH-PA Author Manuscript

Table 1

Summary of mechanical parameters (mean ± SEM) calculated at each testing stage for each biochemical treatment. For stage D, 1 Hz frequency was chosen as representative; cumulative height loss was recorded with respect to the end of stage A. Bold denotes significant difference from control ($p < 0.05$).

Test Stage	Mechanical parameter	Soaked (Control)	Elastase treated	Collagenase treated	Genipin treated
A. Equilibration	d_{inf}–d_0 (mm)	0.82 (0.03)	0.79 (0.05)	0.77 (0.04)	**0.32 (0.03)**
	Time constant τ (s)	2548 (220)	3490 (872)	2275 (501)	2376 (281)
	Stretch constant β	0.61 (0.01)	0.62 (0.05)	**0.65 (0.02)**	**0.70 (0.02)**
B. Cyclic compression-tension	Compressive Stiffness (N/mm)	168 (12)	167 (14)	179 (14)	157 (12)
	Tensile stiffness (N/mm)	58.0 (4.5)	**43.0 (6.4)**	64.4 (4.1)	**33.6 (3.5)**
	Neutral Zone Stiffness (N/mm)	0.32 (0.03)	0.35 (0.03)	0.35 (0.02)	**3.62 (0.90)**
	Neutral Zone Length (mm)	0.92 (0.03)	1.01 (0.07)	**1.07 (0.05)**	**0.38 (0.04)**
	Cumulative Height Loss (mm)	0.01 (0.01)	0.03 (0.01)	0.01 (0.01)	−0.01 (0.02)
C. Quasi-static compression	Quasi-static stiffness (N/mm)	24.2 (1.2)	24.5 (1.1)	24.7 (0.8)	25.7 (2.3)
	Cumulative Height Loss (mm)	0.26 (0.01)	0.28 (0.02)	0.26 (0.0)	0.24 (0.02)
D. Dynamic Compression	Dynamic stiffness (N/mm)	215 (17)	213 (22)	**275 (20)**	198 (10)
	Phase Angle (radians)	0.25 (0.03)	0.32 (0.03)	0.33 (0.05)	0.23 (0.02)
	Cumulative Height Loss (mm)	0.26 (0.01)	0.28 (0.02)	0.26 (0.01)	0.23 (0.02)
E. Creep	d_{inf}–d_0 (mm)	0.31 (0.02)	**0.22 (0.04)**	**0.18 (0.03)**	0.31 (0.03)
	Time constant τ (s)	1434 (98)	1072 (2 0 0)	**848 (1 2 0)**	1416 (1 2 3)
	Stretch constant β	0.89 (0.02)	0.91 (0.03)	0.92 (0.04)	0.91 (0.01)
	Cumulative Height Loss (mm)	0.53 (0.03)	0.50 (0.05)	**0.45 (0.03)**	0.51(0.03)

J Biomech. Author manuscript; available in PMC 2010 December 20.

NIH-PA Author Manuscript

NIH-PA Author Manuscript

NIH-PA Author Manuscript

Table 2

Summary of mechanical parameters (mean ± SEM) calculated at each testing stage for caudal and lumbar IVD. For stage D, 1 Hz frequency was chosen as representative; cumulative height loss was recorded with respect to the end of stage A. Bold denotes significant difference from caudal ($p < 0.05$).

Test Stage	Mechanical parameter	Caudal	Lumbar
A. Equilibration	d_{inf}–d_0 (mm)	0.68 (0.06)	**0.37 (0.03)**
	Time constant τ (s)	3864 (916)	4133 (1568)
	Stretch constant β	0.60 (0.02)	0.59 (0.02)
B. Cyclic compression-tension	Compressive Stiffness (N/mm)	118 (12)	98 (9)
	Tensile stiffness (N/mm)	46.1 (3.7)	42.9 (3.6)
	Neutral Zone Stiffness (N/mm)	0.42 (0.09)	**3.33 (1.16)**
	Neutral Zone Length (mm)	0.82 (0.05)	**0.43 (0.04)**
	Cumulative Height Loss (mm)	0.02 (0.0)	−0.03 (0.02)
C. Quasi-static compression	Quasi-static stiffness (N/mm)	23.86 (1.1)	23.09 (3.0)
	Cumulative Height Loss (mm)	0.27 (0.01)	0.26 (0.03)
D. Dynamic Compression	Dynamic stiffness (N/mm)	145 (21)	102 (11)
	Phase Angle (radians)	0.21 (0.03)	0.19 (0.03)
	Cumulative Height Loss (mm)	0.25 (0.01)	0.23 (0.03)
E. Creep	d_{inf}–d_0 (mm)	0.34 (0.02)	**0.21 (0.06)**
	Time constant τ (s)	1880 (193)	**803 (93)**
	Stretch constant β	0.86 (0.03)	**0.78 (0.03)**
	Cumulative Height Loss (mm)	0.53 (0.02)	0.51 (0.09)

NIH-PA Author Manuscript

NIH-PA Author Manuscript

NIH-PA Author Manuscript

Table 3

Summary of % change in biochemical content of the whole disc (mean± SEM) calculated for each intervention. Collagen content was assessed with a hydroxyproline assay and is expressed here as % change in mg hydroxyproline/mg dry tissue content from control. Collagen crosslinking was assessed with the ninhydrin assay which measures free amino acids. The results are presented as % change in crosslinking from control. GAG content was measured using the 1,9-dimethylmethylene blue (DMMB) assay and the results are presented as % change in GAG content from control. Bold denotes significant difference from control ($p < 0.05$).

Biochemical content	Assay	Elastase treated	Collagenase treated	Genipin treated
Collagen	Hydroxyproline	−23.4 (6.8)	**− 49.9 (18.7)**	NA
Free Amines	Ninhydrin	**37.7 (8.7)**	**123.9 (26.2)**	**− 37.2 (9.2)**
GAG	DMMB	**− 32.0 (5.3)**	**31.1 (4.9)**	NA